Am J Cancer Res 2023;13(5):1904-1922
www.ajcr.us /ISSN:2156-6976/ajcr0146027

Original Article

CXCL10 and CCL5 as feasible biomarkers for immunotherapy of homologous recombination deficient ovarian cancer

Yue Han, Zhewei Guo, Lijuan Jiang, Xinyue Li, Jiahui Chen, Ling Ouyang, Yan Li, Xiaoying Wang

Department of Obstetrics and Gynecology, Shengjing Hospital of China Medical University, Shenyang, Liaoning, China

Received August 19, 2022; Accepted April 27, 2023; Epub May 15, 2023; Published May 30, 2023

Abstract: This study aims to identify biomarkers of ovarian cancer, specifically those tumors exhibiting homologous recombination deficiency (HRD), to contribute to the optimization of immunotherapy. We screened the differentially expressed genes coding for CXCL10 and CCL5 by analyzing the transcriptome data of patient with different HRD scores in the ovarian cancer cohort of the TCGA database and validated our results using pathological tissue sections. The cellular origin of CXCL10 and CCL5 were identified using the single-cell sequencing data extracted from the GEO database combined with the tumor mutational burden (TMB) and single nucleotide polymorphism (SNP) data obtained from the TCGA database. We found that CXCL10 and CCL5 expression levels were correlated with HRD score. Analysis of single-cell sequencing results and tumor mutation data suggested that both CXCL10 and CCL5 present in the tumor microenvironment were primarily derived from immune cells. In addition, we found that samples with high expression of CXCL10 and CCL5 also had higher stromal cell and immune cell scores, indicating low tumor homogeny. Further analysis showed that CXCL10 and CCL5 expression was associated with immune checkpoint-related genes, and the efficacy of using these proteins as biomarkers was significantly higher than that of PD-1 in predicting the effect of anti-PD-1 immunotherapy. The expression of CXCL10 and CCL5 had statistically different effects on the survival of patients, based on multivariate Cox regression. In summary, the results demonstrate that in ovarian cancer, the expression of CXCL10 and CCL5 are correlated with HRD. When CXCL10 and CCL5 are secreted by immune cells, immune cell infiltration can be chemotactic and predict the effect of immunotherapy more efficiently than using PD-1 as a biomarker. Therefore, CXCL10 and CCL5 look to be promising novel biomarkers to guide immunotherapy in ovarian cancer.

Keywords: Ovarian cancer, homologous recombination defects, CXCL10, CCL5, immunotherapy

Introduction

As one of the most prevalent tumors of the female reproductive system, the incidence of ovarian cancer continues to increase in tandem with the aging of our population [1]. Recent advancements in diagnosis, treatment, combination therapies and surgical techniques have provided a good foundation for creating a complete management process for ovarian cancer. The successful use of poly (ADP-ribose) polymerase inhibitors (PARPi) to treat recurrent ovarian cancer in patients with BRCA mutations, first accomplished in 2014, heralded a new era of precise tumor targeting. Studies have shown that homologous recombination deficiency (HRD), caused by BRCA mutations, is strongly corelated with patient prognosis [2-4]. Integrative analysis of the expression profile data of 316 cases and all-exon 489 cases in high-grade serous ovarian cancer revealed that up to 50% of ovarian cancers may have abnormal homologous recombination repair (HRR) pathways [5]. In addition, studies pertaining to pancreatic cancer, as well as small cell lung cancer, have revealed that similar abnormalities in homologous recombination repair pathways exist in a variety of tumors and may respond to treatment with PARP inhibitors [6, 7].

However, homologous recombination repair pathway genes are widely distributed and have complex mechanics. Therefore, the use of HRD

status as a universal marker of cancer is still in its infancy, in terms of clinical application. Furthermore, although some patients initially show a good response to PARPi, it is clear that this treatment does not halt disease progression in a significant number of cases. Therefore, many scholars have applied themselves to investigating the efficacy of PARPi when used in combination with immune checkpoint inhibitors. The therapeutic effects of immune checkpoint inhibitors in patients with either BRCA 1/2 mutated, or HRD-positive ovarian cancer was presented at the American Society of Gynecologic Oncology (SGO) in 2021. The results suggested it is clinically beneficial to supplement PARPi with atezolizumab when treating BRCA1/2 mutated and HRD-positive patients [8]. This result is consistent with the TOPACIO trial [9]. The study used a BRCA1-deficient mouse model and revealed that mice treated with PARPi showed increased expression of PD-L1 and that the survival of mice was further prolonged by administering anti-PD-1 drugs [10]. Therefore, the identification of new immunotherapeutic targets and tumor markers, which can be used in conjunction, offer practical benefits for the treatment of tumors.

Existing studies have shown that PARPi increases cytosolic DNA by inducing fragmentation of double-stranded DNA. Cyclic GMP-AMP synthetase (cGAS) acts as a cytosolic DNA sensor which ultimately activates the stimulator of interferon genes (STING) signaling pathway [11, 12]. The cGAS-STING pathway represents an important part of the innate immune system, as it can stimulate dendritic cells, macrophages, etc., to secrete type I interferon, which in turn activates the innate immune response [13]. In dendritic cells lacking cGAS or STING, innate immune recognition of cancer is defective and the production of tumor-infiltrating CD8+ T cells is impaired. Therefore, activation of the cGAS - STING pathway can induce and promote cross-presentation of tumor antigens, activate T cells, and subsequently perform a tumor monitoring role [14].

In this study, we aim to determine biomarkers that can be used to guide immunotherapeutic treatment of patients with homologous recombination-deficient ovarian cancer. To accomplish this objective, we analyzed the links between HRD scores, transcriptome data, and other relevant immune characteristics of ovarian cancer using records extracted from the TCGA database. CXCL10 and CCL5, the key downstream target genes of the cGAS-STING pathway, have been found to correlate with HRD status. Furthermore, patients with high expression of CXCL10 and CCL5 had survival rates comparable to patients with low expression. Further analysis suggested that the expression of CXCL10 and CCL5 was positively correlated with the immune score of the tumor microenvironment and linked with the infiltration of certain immune cells. More importantly, the analysis of the immunotherapeutic effect shows that CXCL10 and CCL5 have better predictive value than PD-1.

Methods

Data extraction and analysis

The expression profile data of genes and their related clinical attributes data were sourced from the public databases: the Cancer Genome Atlas (TCGA) database (https://portal.gdc.cancer.gov/) and the Gene Expression Omnibus (GEO) database (https://www.ncbi.nlm.nih.gov/geo/). From the former, we downloaded the gene expression profiling data and gene mutation data contained in the TCGA-OV cohort. This yielded a total of 339 samples, of which 96 records were removed due to insufficient information, a total of 243 samples were finally included in the final analysis. In addition, BRCA1-deficient ovarian cancer gene expression profiling data were derived from GSE120500 (https://www.ncbi.nlm.nih.gov/geo/query/acc.cgi?acc=GSE120500), and a total of 12 sample data were extracted from GSE120500 for inclusion in the final analysis. Single-cell sequencing data were obtained from GSE148569 (https://www.ncbi.nlm.nih.gov/geo/query/acc.cgi?acc=GSE148569).

Data related to immunotherapy were derived from the Imvigor210 cohort [15]. When the protein expression level was higher than the mean of all samples, it was considered that the protein was highly expressed. The assessment of pan-cancer data was achieved through the Sangerbox tools, a free-of-charge online platform for data analysis (http://www.sangerbox.com/tool). CXCL10 and CCL5 of different ovarian cancer groups were obtained from TISIDB database. CXCL10 and CCL5 data were obtained from the ovarian cancer datasets con-

tained in the publicly accessible TISIDB database [16]. The HRD score was calculated using the sum of loss of heterozygosity (LOH), Large-scale State Transitions (LST), and Telomeric Allelic Imbalance (TAI) [17]. The HRD score of each sample is displayed in Supplementary Table 1.

Screening of differential genes and enrichment analysis

First, the TCGA-OV cohort samples were ranked by HRD score. Samples in the first and fifth quintiles were selected as study subjects. We analyzed the gene expression data of these samples with the limma package [18] using version 3.6.3 of R [19], then performed differential gene screening using a cut-off value of logFC ≥ 0.5 and *P*-value < 0.05. Gene Ontology (GO) and KEGG pathway enrichment analysis was conducted using the "clusterProfiler" package [20].

Calculation of tumor mutation burden

Tumor mutation burden (TMB) for a specific region of interest is defined as the ratio.

Total number of mutations counted: Length of the coding region [21].

The main mutation types include nonsense mutations, frame-shift deletions, frame-shift insertions, splice sites and missense mutations. In this study, the TMB was determined for 463 samples and the calculations for each sample are documented in Supplementary Table 2.

Single-cell sequencing

The raw data used for single-cell sequencing analysis were derived from GSE148569. A total of 477 samples were included in the final analysis. The data were analyzed by applying the Seurat package [22] using version 3.6.3 of R [19]. The number of gene expressions > 50 and < 5% of mitochondria-related genes was selected as a data filtering condition. Eventually, the top 3000 genes, in terms of the largest fluctuations in gene expression, were selected for the next stage of analysis. Through PCA, TSNE performs dimensionality reduction of the data. The FindClusters function categorized the cells into seven clusters. Gene expression markers for each cell cluster were determined using the FindAllMarkers function and the results used for cell annotation. We used the public database, CellMarker [23] and the Mouse Cell Atlas [24] in conjunction to complete the cell annotation.

Immunohistochemistry

For this analysis, our subject group contained 42 patients with ovarian cancer, who were first diagnosed by Shengjing Hospital of China Medical University, during the period from January 2018 to March 2022, and who had been assigned an HRD score. These patients had had tissue samples collected, which were formalin fixed and paraffin embedded. This study was reviewed and approved by the Ethics Committee. Paraffin slides were dewaxed in xylene and then hydrated in gradient alcohol. After heat-induced antigen repair, the activity of endogenous peroxidase was blocked by adding 3% hydrogen peroxide solution and incubating at room temperature for 10 min. After three rinses phosphate buffered saline (PBS), goat serum albumin was dropped into the solution and incubated at room temperature for 15 min. After dumping the serum, it was mixed with primary antibodies (CXCL10, 1:100, Novus Biologicals (NBP2-67004), USA, CCL5, 1: 20, Invitrogen (710001), USA) and stored overnight at 4°C, then incubated with HRP labeled anti-rabbit IgG (ZSGB-BIO (SP90001-06)) at room temperature for 15 min. The samples were then stained with 3-diaminobenzidine (DAB), followed by hematoxylin. The results were evaluated by two senior pathologists using semi-quantitative evaluation techniques. Given that no significant intratumoral heterogeneity was observed during staining, immunohistochemical assessments of protein expression were solely based on staining intensity: negative (-), weak (+), moderate (++) or strong (+++).

Immune profile analysis

The tumor immune microenvironment was scored using the ESTIMATE package [25] with version 3.6.3 of R [19]. The results were visualized using ggplot2 [26]. Tumor immune cell infiltration analysis was performed using the CIBERSORT function [25] and the subsequent results were visualized with a Vioplot package [27]. We investigated whether the expression of CXCL10 is correlated with common immune checkpoint genes using a combination of the corrplot [28] ggplot2 [26] packages.

Statistical analysis

In this study, survival analysis was performed using GraphPad Prism9.0.2 and ROC curves were plotted. Correlation analysis was performed using the Pearson correlation test. In this study, IBM SPSS statistics 26 was applied for multivariate COX regression analysis. $P < 0.05$ was considered statistically significant.

Results

CXCL10 and CCL5 as the downstream genes of the cGAS-STING pathway is associated with HRD

Data relating to a total of 339 TCGA-OV cohort samples were downloaded from the publicly accessible TCGA database. After 96 samples were excluded due to incomplete data, 243 samples were included in our study. Recent reports suggest that HRD status may play a crucial role in predicting ovarian cancer prognosis [29, 30]. HRD score ≥ 42 is defined as HRD-positive according to the Myriad MyChoice® CDx test platform approved by the FDA. Survival analysis, revealed a statistically significant difference between the HRD-positive and HRD-negative patient groups ($P < 0.05$, Supplementary Figure 1A). Further analysis revealed that HRD score predicted a 5-year survival rate of 61.36% (Supplementary Figure 1B). Thus, our results agreed with previous studies which suggest that HRD status may be a prognostic marker in ovarian cancer. Hence, the above samples were ranked individually, according to HRD scores. The first and fifth quintiles were selected for subsequent studies. The HRD scores of all samples are detailed in Supplementary Table 1. Differential gene expression analysis was performed using the limma package in R [18, 19], with a cut-off value of logFC ≥ 0.5 and *P*-value < 0.05. A total of 450 differentially expressed genes fell within these parameters, consisting of 329 up-regulated and 121 down-regulated genes. The results are presented in a volcano plot (**Figure 1**). KEGG and GO enrichment analysis of these differential genes revealed that the vast majority were associated with the chemokine pathways and to some extent the immune-related signaling pathways, such as chemokine activation and leukocyte migration (**Figure 1**). Interestingly, the chemokines CXCL10 and CCL5 have been implicated in several of these signaling pathways. Existing studies have shown that CXCL10 and CCL5 are the key downstream target genes of the cGAS-STING pathway. The cGAS-STING pathway, as a part of the innate immune system, is abnormally activated in homologous recombination-deficient ovarian cancer [31, 32]. Such findings imply that CXCL10 and CCL5 may be involved in ovarian tumor development. Further analysis supported the theory that there was a co-expression relationship between CXCL10 and CCL5 (**Figure 2A**), and the expression of both was correlated with HRD status (**Figure 2B**, **2C**). In addition, patients with high expression of both CXCL10 and CCL5 exhibited significantly better survival rates compared with those with low expression ($P < 0.05$, **Figure 2D**).

In addition, our analysis of the GSE120500 cohort showed that STING, TBK1, IRF3, and CXCL10 expression was significantly increased in BRCA1-deficient ovarian cancer patients after PARPi treatment compared with controls. Furthermore, CXCL10 expression was strongly correlated with that of STING, TBK1, and IRF3 (**Figure 2E-G**), which have been shown to be key genes of the cGAS-STING pathway [33]. A pan-cancer analysis of CXCL10 expression, using data from the TCGA database on multiple cancer types, indicated that this pattern of differential CXCL10 and CCL5 expression was present in multiple tumors (**Figure 2H**, **2I**). Furthermore, based on these results, we can conclude that, as a downstream gene within the cGAS-STING pathway, CXCL10 is associated with HRD. The differential gene screening process is shown in **Figure 1**.

Immunohistochemical results confirmed that CXCL10 and CCL5 were highly expressed in HRD-positive ovarian cancer

A total of 42 ovarian cancer patients with a known HRD score were enrolled in this study. There were twenty-one HRD-positive patients and twenty-one HRD-negative patients. For each group, the expression of CXCL10 and CCL5 was analyzed via immunohistochemical staining of surgical specimens. The results showed that CXCL10 and CCL5 are expressed in the cytoplasm and membrane. In the HRD-positive cohort, CXCL10 expression was strongly positive in two cases (9.52%, **Figure 3A**), moderately positive in eight cases (38.10%), weakly positive in six cases (28.57%), and negative in five cases (23.81%). Whereas in the HRD-negative cohort, there were two moder-

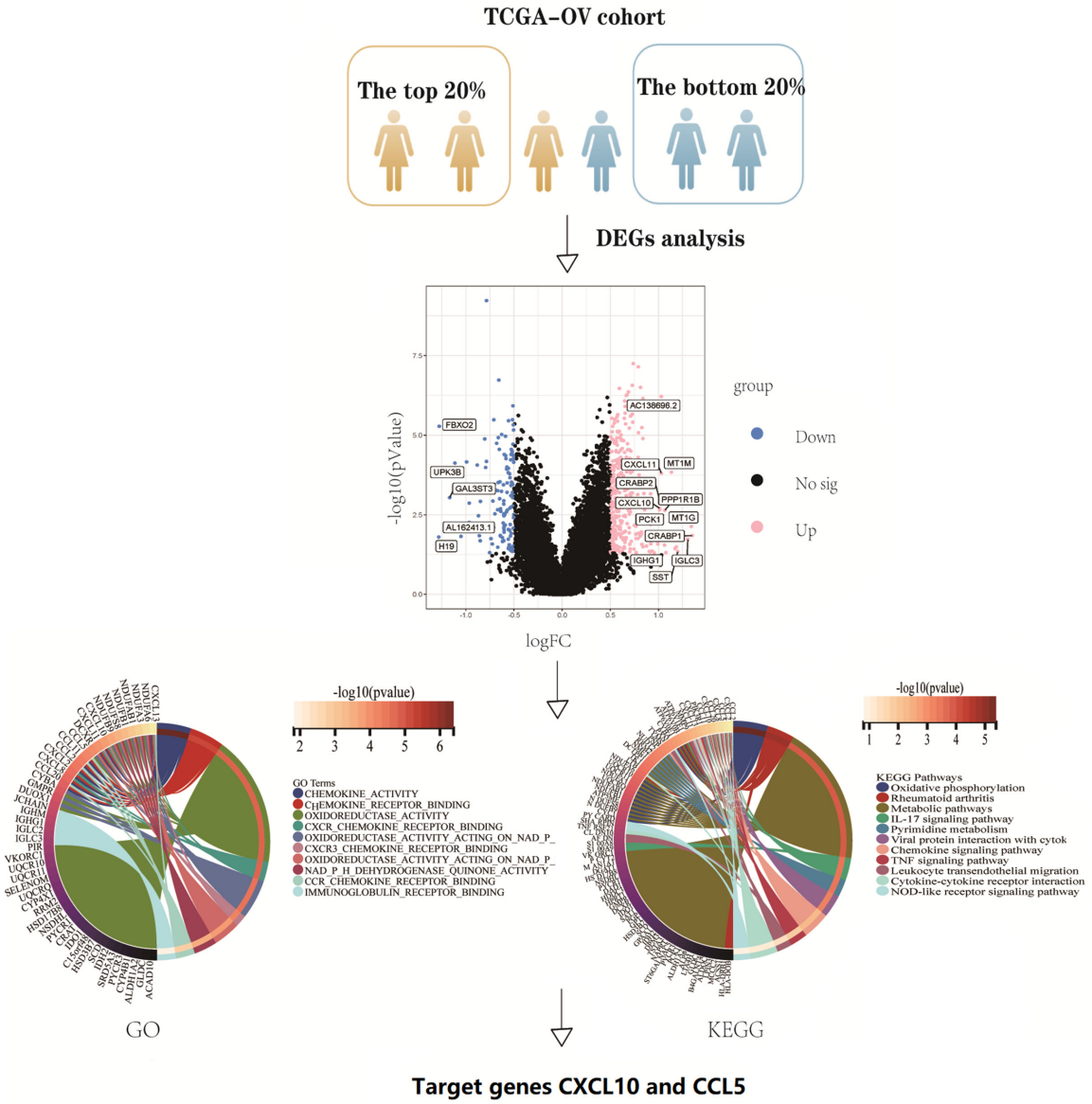

Figure 1. Flow chart of target gene screening. Key genes were screened by comparing the difference in gene expression in the top 20% versus the bottom 20% of samples with HRD scores in the TCGA-OV cohort. Volcano plots showing differential genes selected with logFC ≥ 0.5, *P*-value < 0.05. GO and KEGG plots show the results of differential genes enrichment analysis.

ately positive patients (9.52%), three weakly positive patients (14.29%), and sixteen negative patients (76.19%, **Figure 3B**). Chi-square analysis showed that CXCL10 expression was significantly different between the two groups (P < 0.05, **Figure 3E**). Analysis of CCL5 expression showed that in HRD-positive patients: three cases were strongly positive (14.29%, **Figure 3C**), nine cases were moderately positive (42.86%), five cases were weakly positive (23.81%), and four cases were negative (19.04%). However, among the twenty-one HRD-negative patients, one was strongly positive (4.77%), four were moderately positive (19.04%), four were weakly positive (19.04%), and twelve were negative (57.15%, **Figure 3D**). Chi-square analysis showed that the expression of CCL5 was significantly different between the two groups (P < 0.05, **Figure 3F**). Therefore, immunohistochemical results indicate that CXCL10 and CCL5 are often overexpressed in HRD-positive ovarian cancer.

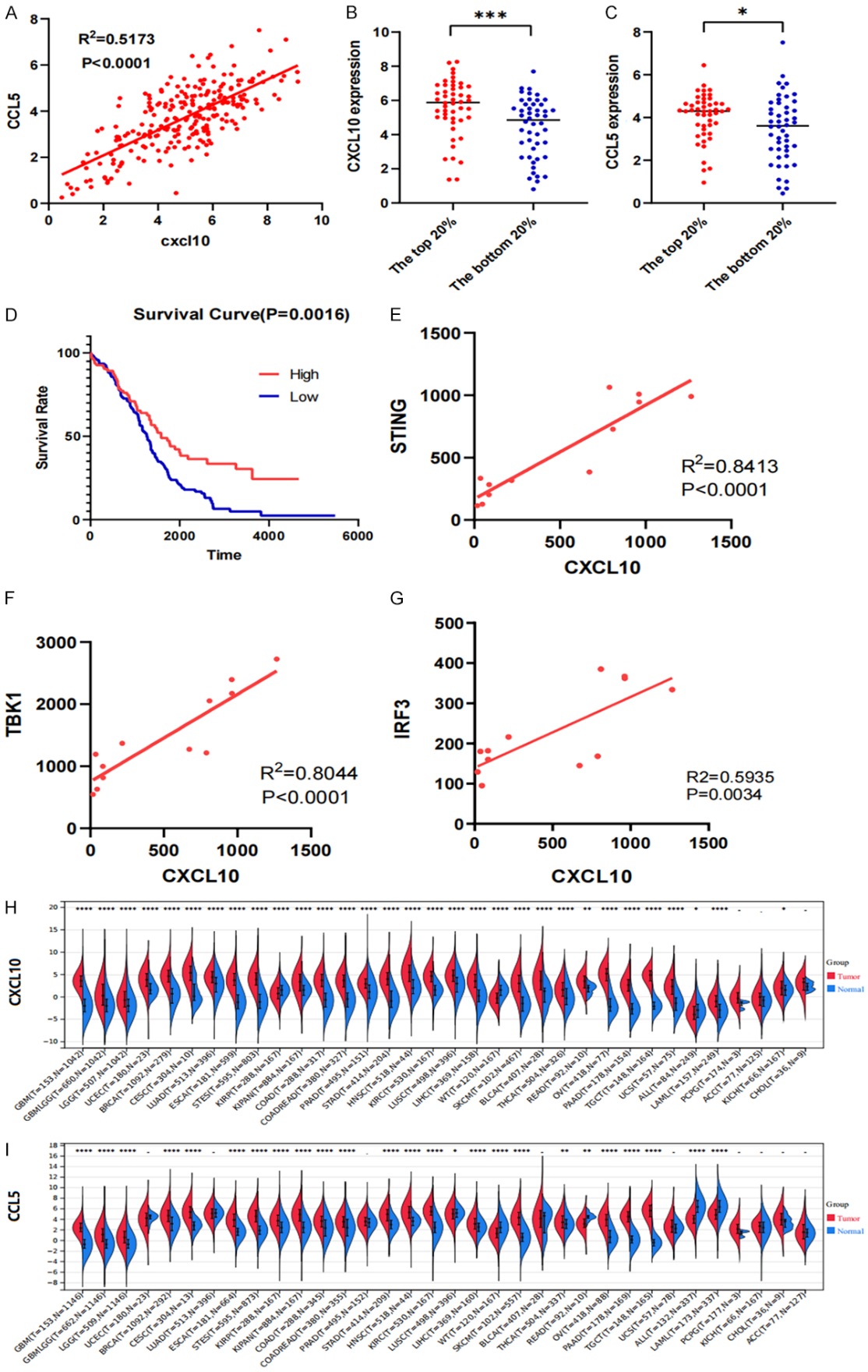
A
R²=0.5173
P<0.0001
CCL5
cxcl10
B
***
CXCL10 expression
The top 20%
The bottom 20%
C
*
CCL5 expression
The top 20%
The bottom 20%
D
Survival Curve(P=0.0016)
High
Low
Survival Rate
Time
E
STING
R²=0.8413
P<0.0001
CXCL10
F
TBK1
R²=0.8044
P<0.0001
CXCL10
G
IRF3
R2=0.5935
P=0.0034
CXCL10
H
CXCL10
Group
Tumor
Normal
I
CCL5
Group
Tumor
Normal

Figure 2. As the downstream genes of the cGAS-STING pathway, CXCL10 and CCL5 are associated with HRD. A. Scatter Plot of Correlation Between CXCL10 and CCL5 Expression in TCGA-OV Cohort. B and C. CXCL10 and CCL5 were expressed in the top 20% group and the bottom 20% of HRD score. D. Survival curves for high versus low expression of CXCL10 and CCL5 in the TCGA-OV cohort. E-G. Scatterplot of the correlation between STING, TBK1, IRF3 and CXCL10 expression in ovarian cancer patients treated with PARPi in the GSE120500 cohort. H. Violin plot of CXCL10 expression in a variety of tumor tissues versus normal tissues. I. Violin plot of CCL5 expression in a variety of tumor tissues versus normal tissues.

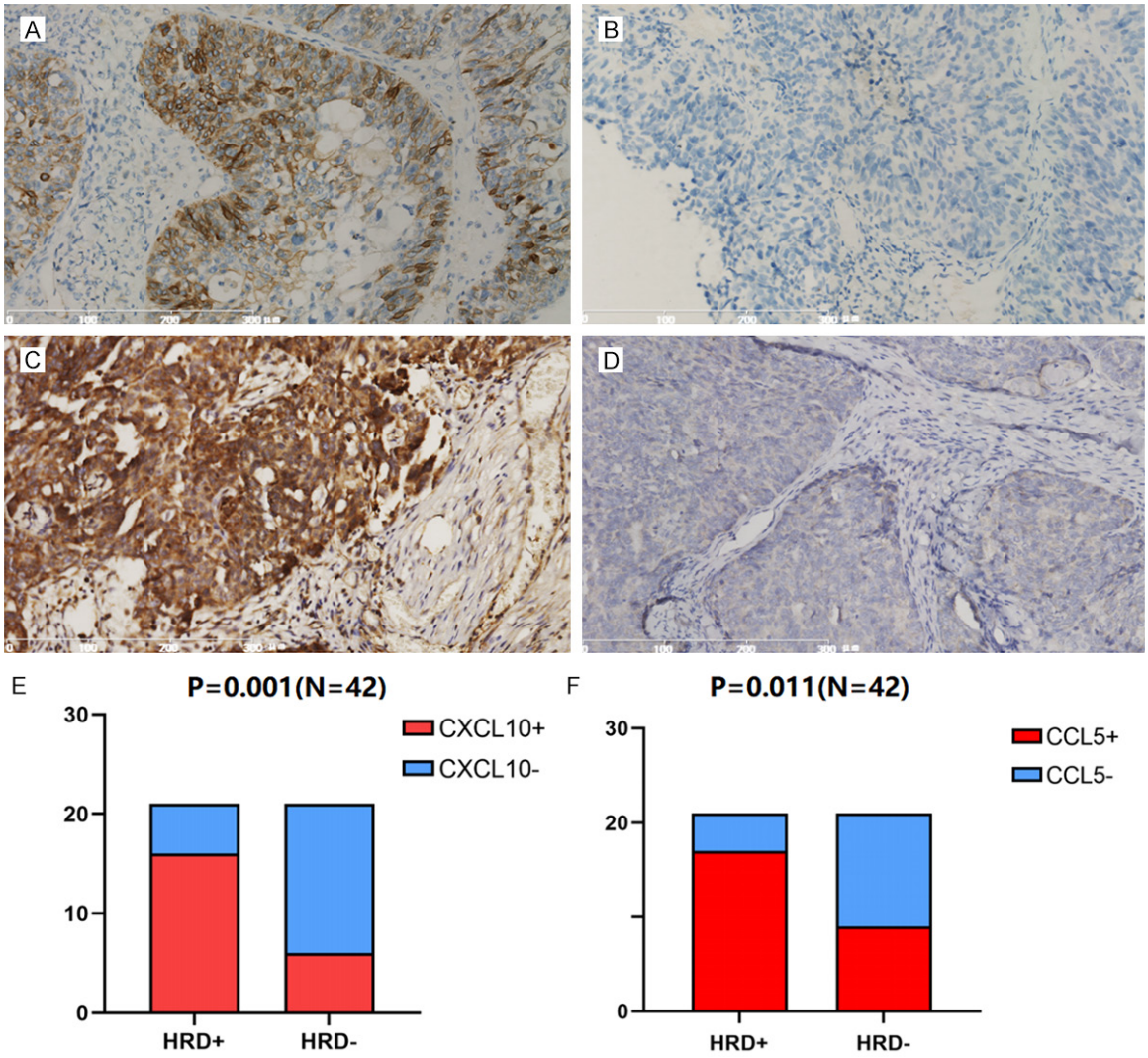

Figure 3. Immunohistochemical results confirmed that CXCL10 and CCL5 were highly expressed in HRD-positive ovarian cancer. A. The positive expression of CXCL10 in ovarian cancer showed that the positive expression of CXCL10 was located in the cytoplasm and membrane. B. Negative expression of CXCL10 in ovarian cancer. C. The positive expression of CCL5 in ovarian cancer showed that the positive expression of CCL5 was located in the cytoplasm and membrane. D. Negative expression of CCL5 in ovarian cancer. E and F. Histogram of CXCL10 and CCL5 expression differences in HRD-positive and HRD-negative ovarian cancer patients.

Single cell sequencing results suggested the origin of CXCL10 and CCL5 in the tumor microenvironment

To further clarify the cellular origin of CXCL10 and CCL5 found in the tumor microenvironment, we selected a total of 477 BRCA1-deficient mouse mammary cancer samples GSE148569 cohort for single-cell sequencing analysis. The Seurat package was used for assessment of sequencing data. In the data pre-processing stage, cells with gene expres-

sion numbers less than 2000 were filtered out, and cells with more than 5% mitochondria-related genes were also excluded. Eventually, the top 3000 highly variable genes were selected for PCA, as well as being subjected to the t-SNE algorithm for dimensionality reduction of the data (**Figure 4A**). PCA divided the samples into 15 different PCs, of which 14 PCs had a *P*-value < 0.05 (**Figure 4B**). At the t-SNE dimensionality reduction stage, the samples ended up in seven different cell clusters (**Figure 4C**). Each cell cluster was annotated by screening for marker genes and combination with data from the public database Cell Marker [23] and the Mouse Cell Atlas [24] (**Figure 4D** and Supplementary Table 3). The types of cells in the seven clusters were determined to be: alveolar, endothelial, T-cell, mast, macrophage cells, dendritic and fibroblast; *i.e.* predominantly immune-related (**Figure 4E**). When each cluster was subject to expression analysis and the results compared, they revealed that CXCL10 mainly originated from immune-related cells, such as macrophages, dendritic cells and T cells (**Figure 4F**); whereas for CCL5, it was mainly macrophages and dendritic cells (**Figure 4G**). This suggests that CXCL10 and CCL5 were mainly derived from immune-related cells in the tumor microenvironment and may play a role in tumor-related immune response.

To investigate other sources of CXCL10 and CCL5 in the tumor microenvironment, we analyzed the gene mutation data from the TCGA-OV cohort. After calculating the TMB for each sample, we tried to ascertain if there was any correlation between the expression of CXCL10 and CCL5 with regards to TMB. The results showed that there was a small correlation (R = 0.16, P = 0.034) between CXCL10 expression and TMB (**Figure 4H**), but there was no correlation between CCL5 expression and TMB (P > 0.05, **Figure 4I**). At the same time, we also investigated the relationship between single nucleotide polymorphisms (SNP) and CXCL10 and CCL5 expression independently, in order to further clarify their source. In both comparisons, gene expression was found to be independent of SNP in all of the samples that had measured both gene expression data and SNP data (Supplementary Table 4). These results support our earlier findings which suggest that CXCL10 and CCL5 are mainly derived from immune-related cells in the tumor microenvironment and may play a role in tumor-related immune responses.

High expression of CXCL10 and CCL5 are related with the immune profile of the tumor microenvironment

Current studies suggest that multiple chemokines play key roles in orchestrating tumor immunity [34, 35]. Therefore, in this study, the ESTIMATE algorithm [25] was used to perform stromal, immune and ESTIMATE scoring for samples exhibiting CXCL10 or CCL5 expression. The purpose of this analysis was to obtain tumor microenvironment characteristics related to expression, such as stromal cell score, degree of immune cell infiltration and tumor purity. Compared with the low expression group, the high expression group of CXCL10 and CCL5 had statistically significantly higher (all P < 0.001) stromal scores (P < 0.001, **Figure 5A**), immune scores and ESTIMATE scores (**Figure 5A-C**). Further analysis of the relationship between different immune cells in the tumor microenvironment and CXCL10 expression showed that CD8+ T cells (P < 0.05), activated CD4+ T cells (P < 0.001), M1 macrophages (P < 0.001), and activated dendritic cells (P < 0.05) were related with CXCL10 expression (**Figure 5D**). Dendritic cells, M1 macrophages, M2 macrophages, activated CD4+ T cells, CD8+ T cells, and Treg cells were correlated with CCL5 expression (P < 0.05, **Figure 5D**). Subsequently, we repeated our analysis of the data from the TIMER database [36], which showed that CXCL10 expression was positively correlated with dendritic cells, M1 macrophages, NK cells, CD8+ T cells, memory B cells, and activated CD4+ T cells, but negatively correlated with mast cells, M0 macrophages, eosinophils, and naive B cells (**Figure 5E**). Interestingly, the correlation between CXCL10 expression and dendritic cells exceeded 0.7 (P < 0.001, **Figure 5F**) and similarly with M1 macrophages exceeded 0.5 (P < 0.001, **Figure 5F**). These findings are consistent with our results from single-cell sequencing. Furthermore, we observed a clear correlation between CCL5 expression and M1 macrophages (P < 0.001, **Figure 5F**), but a negative correlation with M0 macrophages and M2 macrophages (**Figure 5F**), suggesting that CCL5 may be involved in the polarization of macrophages. Moreover, recent studies have

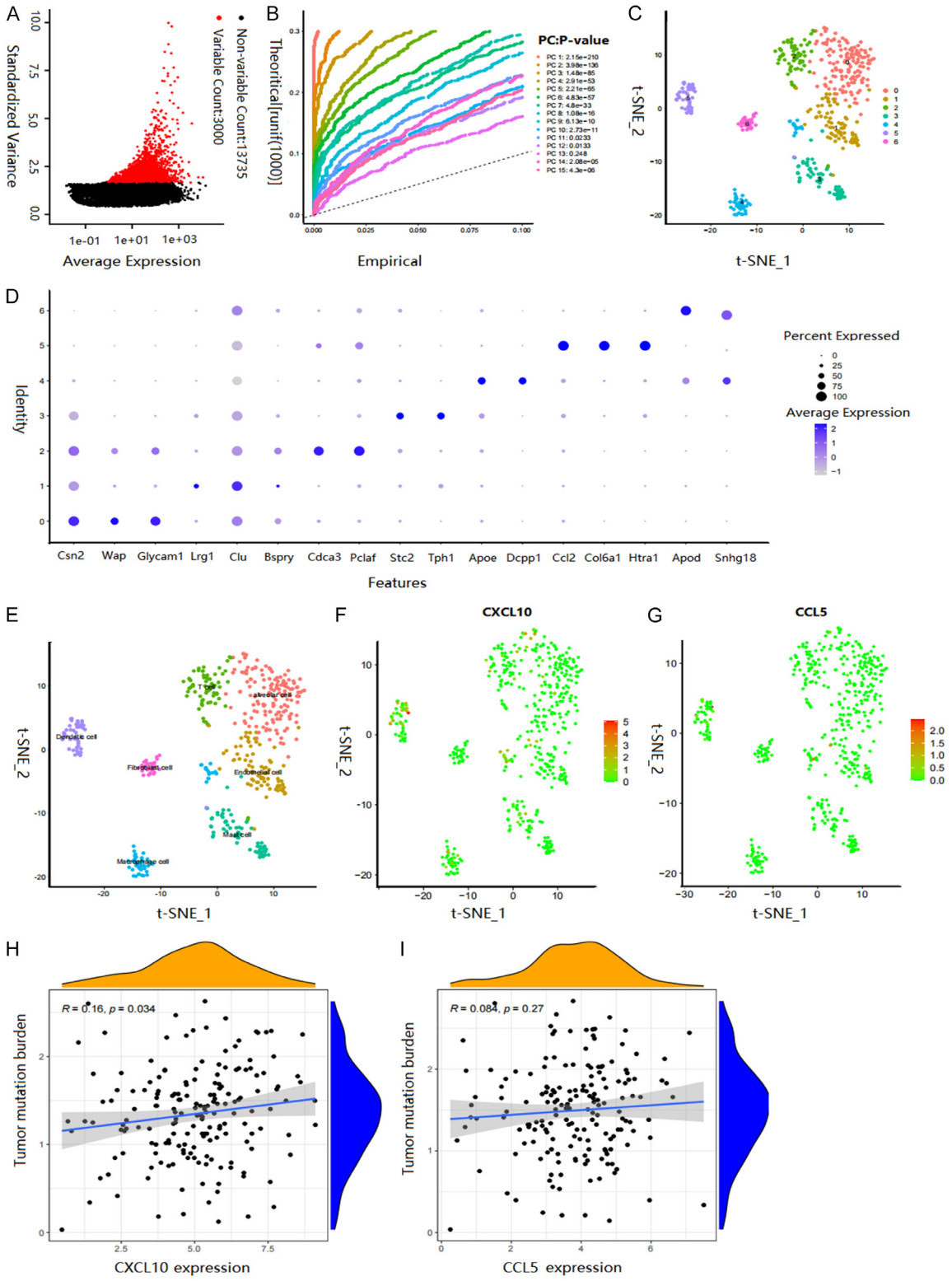

Figure 4. Single cell sequencing results suggested the origin of CXCL10 and CCL5 in the tumor microenvironment. A. Genes were expressed in all samples. Red dots indicate the top 3000 genes with the greatest difference in gene expression. B. PCA principal component analysis plots. C. TSNE Cluster Analysis Diagram. D. Marker Gene Bubble Plot for Different Clusters of Cells. E. Plots annotated to cell clusters. F and G. Scatterplot of CXCL10 and CCL5 expression in different cell clusters. H and I. Scatterplot of the correlation between CXCL10 and CCL5 expression and TMB.

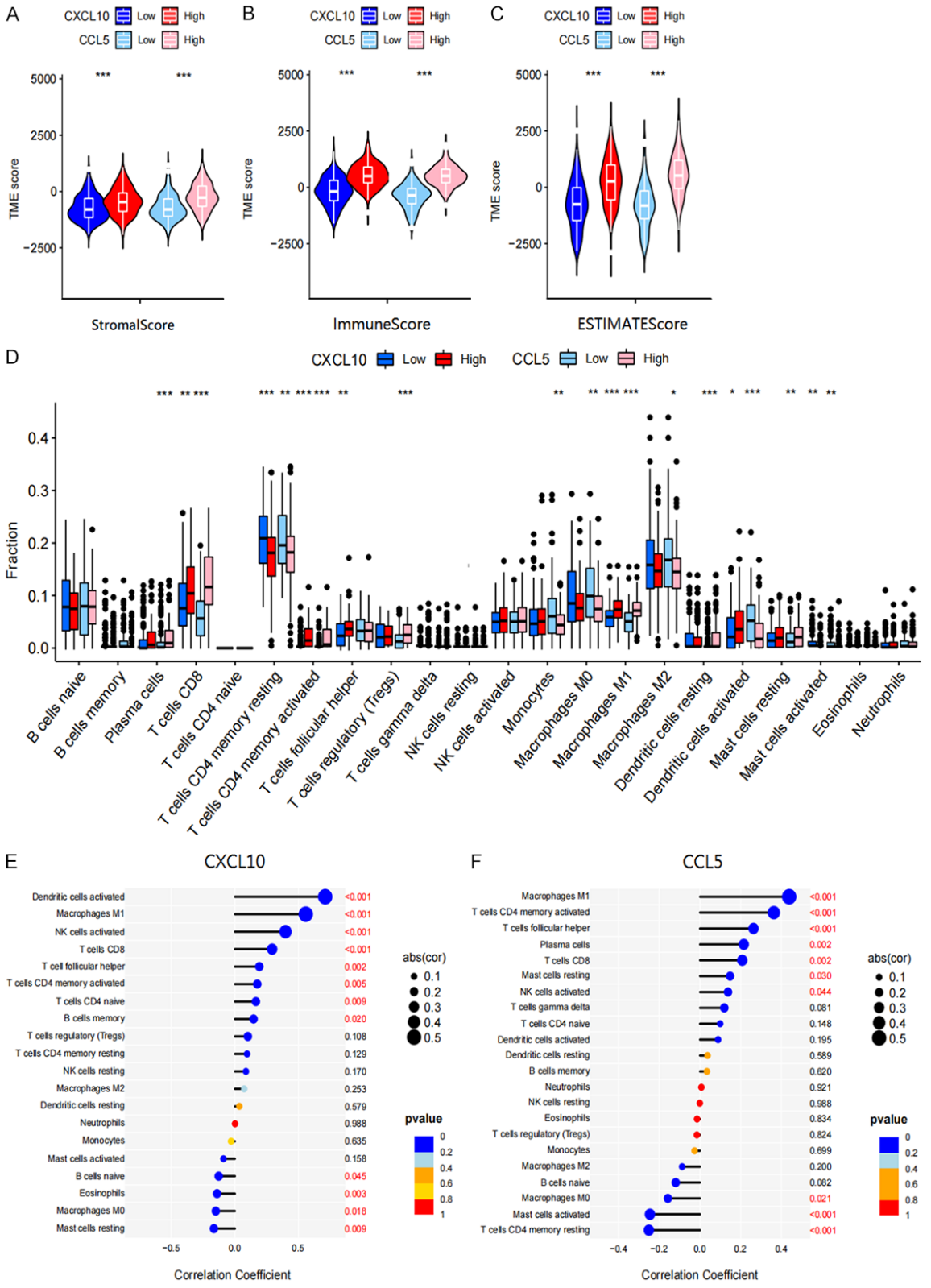

Figure 5. High expression of CXCL10 and CCL5 correlate with the immune profile of the tumor microenvironment. A-C. Stromal score, immune score, and ESTIMATE score in the group with high and low expression of CXCL10 and CCL5 in the TCGA database. D. Box diagram of immune cell difference analysis in the group with high and low expression of CXCL10 and CCL5. E and F. CXCL10 and CCL5 expression in the TCGA database in relation to different immune cells in the tumor microenvironment.

shown that macrophage polarization plays a key role in the development of tumors, with M1 macrophages exhibiting mainly anti-tumor effects, while M2 macrophages exhibit tumor-promoting effects [37, 38]. Importantly, activated M1 macrophages express Th1 chemokines such as CXCL10 to induce immune infiltration, contributing to the formation of the tumor microenvironment. The above results indicate that CXCL10 and CCL5 expression correlate with the immune characteristics of the tumor microenvironment and may play a role in anti-tumor immunity in ovarian cancer.

Correlation of CXCL10 and CCL5 expression with a variety of immune checkpoint-related genes

Immune checkpoints play a key role in maintaining immune tolerance as well as regulating the type of immune response. This makes them ideal targets for those developing novel immunotherapies for the treatment of cancer [39]. Therefore, in this study, we looked for patterns with co-expression between either CXCL10 or CCL5 and more than 30 common immune checkpoint-related genes to clarify their application value in ovarian cancer. As shown in the heatmap (**Figure 6A**), CXCL10 expression showed correlation with a variety of immune checkpoint-related genes. Using a cut-off of correlation coefficient > 0.6, we were able to identify thirteen immune checkpoint-related genes (LAIR1, LAG3, ICOS, CTLA4, CD48, HAVCR2, CD80, LGALS9, IDO1, PDCD1LG2 (PD-L2), TIGIT, CD274 (PD-L1) and CD86) that appear to have a strong correlation with CXCL10. Similarly, more than ten immune checkpoint-related genes were significantly correlated with CCL5 expression ($P < 0.001$, **Figure 6B**), of which CD48, CD86, HAVCR2, LAIR1, TIGIT, CD27, PDCD1LG2, ICOS and CTLA4 had correlation coefficients > 0.7 with CCL5 expression. CD274 ($P < 0.001$, **Figure 6C**, **6F**), PDCD1 (PD-1) ($P < 0.001$, **Figure 6D**, **6G**) and CTLA4 ($P < 0.001$, **Figure 6E**, **6H**), as the most useful immune checkpoint-related genes in clinical practice, were positively correlated with both CXCL10 and CCL5 expression. A recent study showed that BTNL2 is able to directly inhibit the activation of CD4+ T cells. Furthermore, patients with tumors with low BTNL2 expression had significantly improved survival. Curiously, in our study we concluded that CXCL10 and CCL5 expression were inversely correlated with BTNL2 [40]. In summary, we found CXCL10 and CCL5 were significantly correlated with a variety of immune checkpoint-related genes in ovarian cancer and could be used as novel biomarkers to predict the outcome of immune checkpoint blocking therapy.

CXCL10 and CCL5 as feasible markers to predict the efficacy of cancer immunotherapy

As soon as immunotherapy was proven successful for the treatment of certain types of tumors, researchers began focusing attention on identifying markers capable of predicting the effects of this type of therapy. Our previous studies demonstrate that CXCL10 and CCL5 may play a role in the immune microenvironment of tumors. Therefore, to further clarify the value of these two genes in cancer immunotherapy, we analyzed 348 patients (documented in the Imvigor210 cohort) to assess their response to anti-PD-1 therapy. The results showed that the expression of CXCL10 and CCL5 were statistically different between the responder group and the non-responder group, being higher in the former ($P < 0.001$, **Figure 7A**, **7B**). Further analysis showed that patients with high CXCL10 and CCL5 expression had better survival rates in this immunotherapy cohort ($P < 0.01$, **Figure 7C**). By comparing the combination of CXCL10 and CCL5 expression with PD-1 expression for predicting the effect of immunotherapy, we found that the former had higher predictive efficacy than PD-1, with an AUC of 63.87% (95% CI: 56.89%-70.84%, $P < 0.001$, **Figure 7D**). A multivariate Cox proportional hazards model was constructed that included gender, race, immune phenotyping, TCGA subtype, PD-1 expression, CXCL10 and CCL5 expression. The results showed that CXCL10 and CCL5 expression had a statistically significant effect on survival time (HR = 1.575, 95% CI: 1.045-2.373, $P = 0.03$, **Table 1**). Subsequently, we analyzed data associated with ovarian cancer patients obtained from the TISIDE database [16] and assigned each patient to one of four different prognostically different subgroups based on tumor characteristics: differentiated, immunoreactive, interstitial, and proliferative. The results showed that the expression of CXCL10 and CCL5 were significantly different among these four groups. In addition, the expression of CXCL10 and CCL5

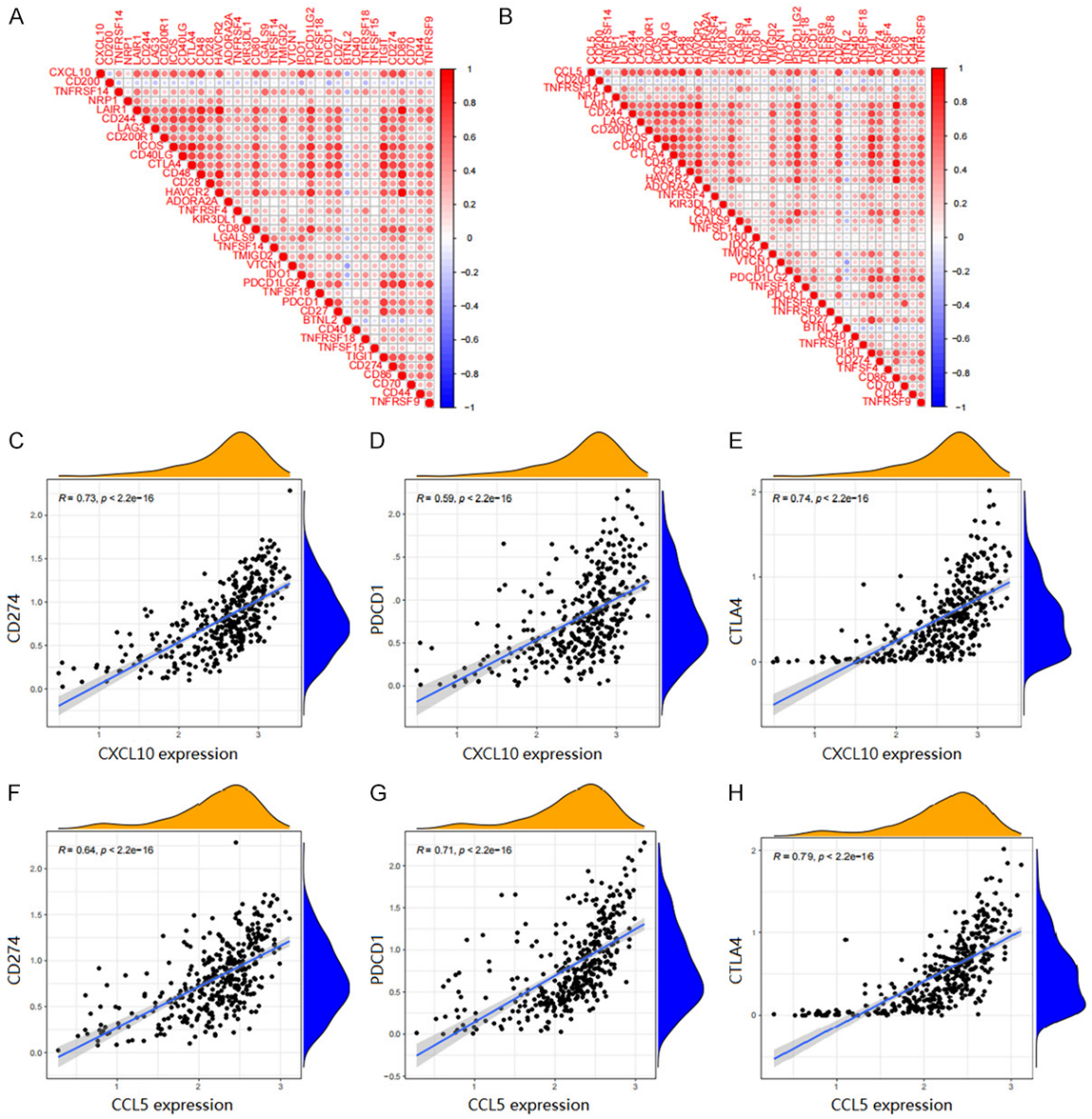

Figure 6. Correlation of CXCL10 and CCL5 expression with a variety of immune checkpoint-related genes. A and B. Heat map of CXCL10 and CCL5 association with immune checkpoint-related genes. C-E. Correlation plot of CXCL10 with CD274, PDCD1, and CTLA4 expression. F-H. Correlation plot of CCL5 with CD274, PDCD1 and CTLA4 expression.

were the highest in patients assigned to the immunoreactive group (**Figure 7E**, **7F**). Furthermore, our analysis revealed that patients in the immunoreactive group showed significant T-cell infiltration and higher survival rates than other groups [41]. Overall, our results indicate that the combination of CXCL10 and CCL5 is superior to PD-1 in predicting the effect of cancer immunotherapy, making it an interesting candidate biomarker for use with cancer immunotherapy.

Discussion

Ovarian cancer, considered the most malignant gynecological tumor, has invisible onset and no noticeable symptoms in the early stage. Thus, most patients are actually in advanced stages of the disease at the time of initial diagnosis. Approximately 25% of ovarian cancers are caused by genetic mutations. In normal cells, DNA damage continues to occur, which unless repaired in a timely fashion, can accu-

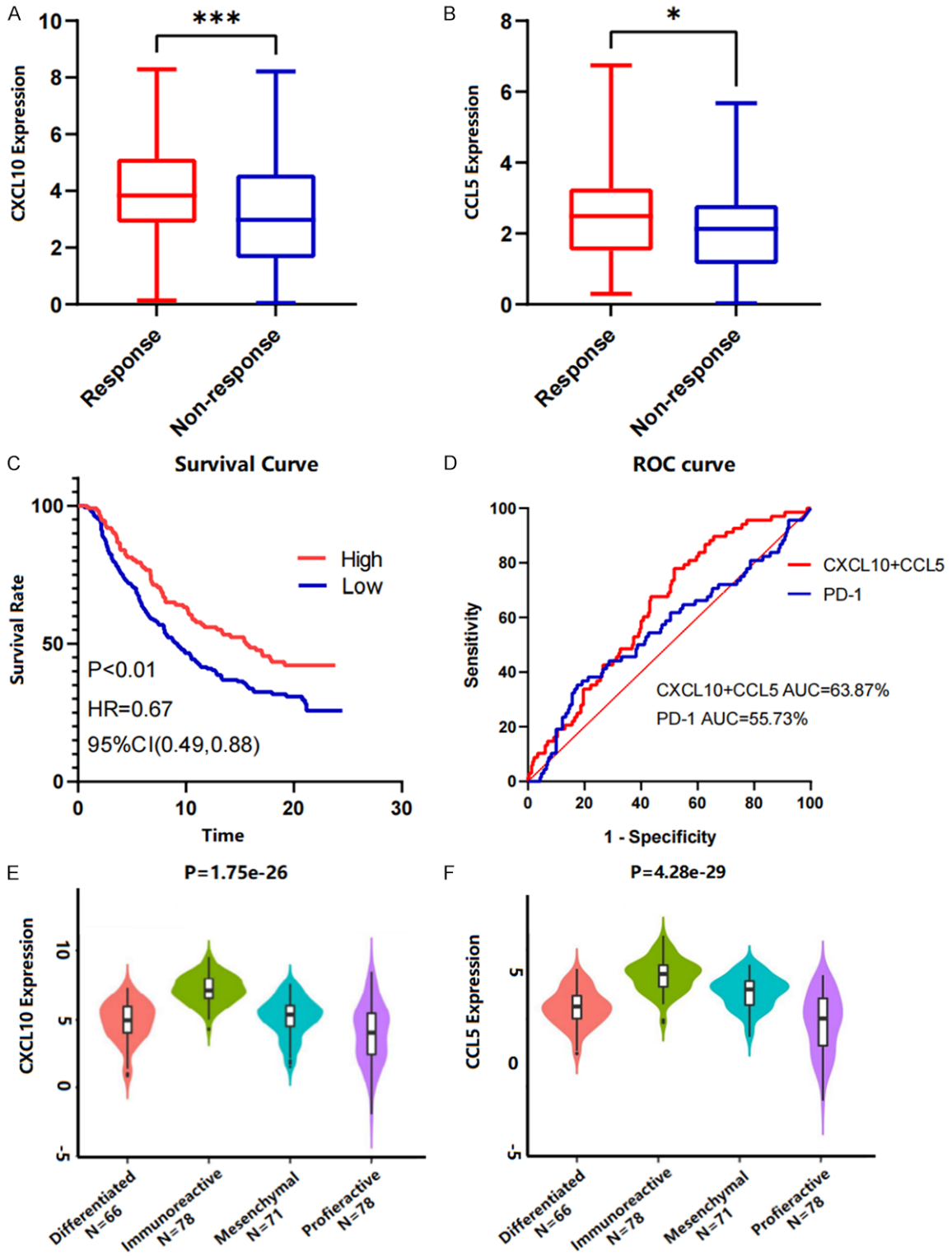

Figure 7. CXCL10 and CCL5 as feasible markers to predict the efficacy of cancer immunotherapy. A and B. Box plots of CXCL10 and CCL5 expression in the immune response group versus the non-response group in the IMvigor210 cohort. C. Survival curves for high versus low expression of CXCL10 and CCL5 in the IMvigor210 cohort. D. ROC curves for CXCL10 and CCL5 versus PD-1 in the IMvigor210 cohort. E and F. Violin plot of CXCL10 versus CCL5 expression in different types of ovarian cancer in the TISIDB database.

Table 1. Multivariate cox regression analysis of IMvigor210 cohort

Variable	Group	N	B	SE	Wald	P	HR	95% CI
Sex								
	female*	59						
	male	221	-0.198	0.175	1.279	0.258	0.82	0.582-1.157
Race								
	white*	257						
	black	15	-0.396	0.388	1.043	0.307	0.673	0.315-1.439
	other	8	-0.718	0.508	1.996	0.158	0.488	0.18-1.321
Immune phenotype								
	excluded*	132						
	desert	75	-0.007	0.18	0.001	0.969	0.993	0.698-1.413
	inflamed	73	-0.282	0.203	1.922	0.166	0.755	0.507-1.124
TCGA Subtype								
	I-II*	110						
	III-IV	170	-0.223	0.155	2.077	0.149	0.8	0.591-1.083
PDCD1								
	HIGH*	111						
	LOW	169	-0.224	0.199	1.267	0.26	0.8	0.542-1.18
CXCL10+CCL5								
	HIGH*	104						
	LOW	176	0.454	0.209	4.717	0.03	1.575	1.045-2.373

"*": Control group.

mulate until the mutations become harmful. Homologous recombination repair is a key signaling pathway for achieving double-stranded DNA break repair. About 50% of serious high-grade ovarian cancers have homologous recombination repair defects, combined with the rapid proliferation of tumor cells causing increasing damage to DNA and subsequent leakage into the cytoplasm. Once detected, the leakage is detected by cGAS, which activates the cGAS-STING pathway, leading to the innate immune response being triggered [42, 43]. Recent studies have shown that genomic instability caused by both homologous recombination defects and mismatch repair defects can: activate the cGAS-STING pathway; create type I interferons and related cytokines [31, 44]; induce immune infiltration and exerts antitumor immune effects. Immune checkpoint blocking therapy may further enhance this cascade and its effects, which could be harnessed to provide a novel approach for treating ovarian cancer. Therefore, in this study, we characterize the immune profile of the tumor microenvironment by analyzing the HRD status of ovarian cancer patients. We also searched for differentially expressed genes that have the potential to act as novel biomarkers that can be used to guide immunotherapy in ovarian cancer exhibiting homologous recombination repair defects.

Based on different HRD scores, we selected 450 differentially expressed genes and identified their biological functions/related pathways using enrichment analysis. Our results revealed a high percentage of these genes coded for chemokines, forming part of immune-related pathways. Concurrently, we found that CXCL10 and CCL5, the major downstream target genes of the cGAS-STING pathway, are positively correlated with HRD. In addition, we observed that the group of patients with high CXCL10 and CCL5 expression had better overall survival rates. Moreover, we found that the expression of STING, TBK1, IRF3, and CXCL10 in HRD-positive ovarian cancer patients, after treatment with PARPi, was significantly increased compared with the control group. We also determined that CXCL10 expression is strongly correlated with the expression of STING, TBK, 1 and IRF3 (these three have been proven to be vital genes of the cGAS-STING pathway) [33, 45]. It has been shown that in HRD-positive

ovarian cancer, PARPi-induced increase in damaged DNA activates the cGAS-STING-TBK1-IFR3-CXCL10 innate immune pathway. Shen, J demonstrated *in vitro* that the mRNA of both CXCL10 and CCL5 increased in tumor cells in a time-dependent manner subsequent to PARPi treatment. Furthermore, this up-regulation of CXCL10 with CCL5 gradually decreased after the knockdown of STING, TBK1, and IRF3 [31].

Tumor heterogeneity is one of the characteristics of neoplasms [46]. Single-cell sequencing reveals tumor heterogeneity by untargeted quantitative detection of transcriptomes in individual cells, as well as identifying ubiquitous transcriptomic states with specific transcriptomes to help gain insight into tumor microenvironment characteristics and thus implement precision therapy [47]. In this study, we analyzed single-cell sequencing data from the GSE148569 cohort to identify the cell types in the tumor microenvironment from which CXCL10 and CCL5 originate. The results of our cell clustering and annotation analyses demonstrated that CXCL10 is mainly derived from macrophages, dendritic cells, and T cells, whereas CCL5 is primarily derived from macrophages and dendritic cells. In order to avoid alteration of CXCL10 and CCL5 transcriptional characteristics due to gene mutation, the gene mutation data of the TCGA-OV cohort were further analyzed in this study to assess the correlation between TMB, SNP and CXCL10/CCL5 expression in the samples. The results showed no correlation, except for CXCL10 expression and TMB ($P < 0.05$). However, in this case, the correlation coefficient is only 0.16, thus it is of little clinical significance and may be ignored. In summary, the results indicate that CXCL10 and CCL5 are mainly derived from immune cells in the tumor microenvironment and may be involved in tumor-related immune responses.

Tumor microenvironment refers to the local environment in which tumor cells grow and develop. In addition to tumor cells, it also contains immune cells, fibroblasts, stromal cells and capillaries. Studies have shown that the tumor microenvironment provides everything necessary for the occurrence, development and metastasis of tumors [48]. By modulating the tumor microenvironment, it is possible to improve the effects of targeted therapeutic agents. Therefore, this study analyzes the relationship between CXCL10 versus CCL5 expression profiles and the tumor microenvironment in the TCGA-OV cohort. High expression of CXCL10 and CCL5 were found to be correlated with higher stromal cell scores and immune cell scores, suggesting that the sample tumors exhibited less tumor purity. Studies have shown that stromal cells, in conjunction with immune cells, can regulate components of the tumor microenvironment and promote metabolic remodeling of tumor cells [49]. In addition, CXCL10 expression was significantly correlated with CD8+ T cells, CD4+ T cells, and dendritic cells. Studies by Mowat demonstrated that the recruitment and activation of CD8+ T cells depends on the overexpression of CXCL-10 and CCL5, and the synergistic effect between CCL5 and IFNγ-induced CXCR3 ligands (CXCL9/10) secreted by bone marrow cells is key to orchestrating T cell infiltration in immunoreactive tumors [34, 44]. Spranger, using flow cytometry and *in vivo* imaging, proposed that the complete inhibition of CXCL10 expression in CD103+ dendritic cells would result in the failure of effector T cells to recruit to the tumor [50]. In fact, the infiltration of a sufficient number of lymphocytes, such as CD8+ T cells and CD4+ T cells, largely determines the efficacy of most targeted drugs.

As a tumor develops, its microenvironment usually evolves in composition to ensure the survival of the tumor cells. In addition, the activation of immune checkpoint pathways can enable tumor cells to evade detection/attack from host defence mechanisms. Some immune checkpoint blocking drugs can re-induce antitumor immunity and promote the elimination of tumors [49]. In this study, we found that CXCL10 and CCL5 were significantly correlated with PD-1/PD-L1 and CTLA4 which are currently the most widely used in clinical practice and in the anti-PD-1 therapy cohort, patients in the responsive group had high CXCL10 and CCL5 expression and good survival rates. When comparing the value of CXCL10 and CCL5 with PD-1 in predicting the efficacy of immunotherapy, we were surprised to find that CXCL10 and CCL5 could replace PD-1 as biomarkers for predicting therapeutic efficacy. Similarly, multivariate Cox regression analysis showed CXCL10, along with CCL5, to be an independent factor for survival. Chow investigated the RNA and protein levels of CXCL9 and CXCL10 and dem-

onstrated that they were significantly increased in tumors following anti-PD-1 therapy. They also determined that the effectiveness of anti-PD-1 therapy was significantly reduced if monoclonal antibodies against CXCL9 and CXCL10 were administered [51]. In tumor-bearing mice treated with anti-PD-1, CXCR3 and its ligands (CXCL9/10) are essential in the process of CD8+ T cell action, and anti-PD-1 treatment is achieved through CXCR3 expression by CD8+ T cells. By examining the expression levels of CXCL9 and CXCL10 in antigen-presenting cells (dendritic cells) sourced from various solid tumors with different response efficiencies to anti-PD-1, it was found that the expression of CXCL10 in anti-PD-1-responsive tumors was significantly increased compared with anti-PD-1-resistant tumors [51]. However, in homologous recombination-deficient tumors with unstable genomes, the mechanics by which CXCL10 and CCL5, present in the tumor microenvironment, regulate anti-tumor immunity needs to be validated with additional *in vivo* and *in vitro* studies. This represents one of the limitations of this study. In addition, much of our data is derived from public databases, so there may be a certain degree of bias in the data collection stage.

Conclusion

In summary, the results demonstrate that in homologous recombination-deficient tumors, the CXCL10 and CCL5, the key downstream target genes of the cGAS-STING pathway, are correlated with HRD score. When CXCL10 and CCL5 are secreted by immune cells in the tumor microenvironment, immune cell infiltration can be chemotactic and can be used to predict the effect of immunotherapy instead of PD-1. Therefore, it is anticipated that future studies will confirm that CXCL10 and CCL5 can be useful biomarkers to guide immunotherapy in homologous recombination-deficient ovarian cancer.

Disclosure of conflict of interest

None.

Address correspondence to: Drs. Yan Li and Xiaoying Wang, Department of Obstetrics and Gynecology, Shengjing Hospital of China Medical University, Shenyang, Liaoning, China. E-mail: leeyan8888@yeah.net (YL); Weibaby44525@sj-hospital.org (XYW)

References

[1] Webb PM and Jordan SJ. Epidemiology of epithelial ovarian cancer. Best Pract Res Clin Obstet Gynaecol 2017; 41: 3-14.

[2] Moore KN, Secord AA, Geller MA, Miller DS, Cloven N, Fleming GF, Wahner Hendrickson AE, Azodi M, DiSilvestro P, Oza AM, Cristea M, Berek JS, Chan JK, Rimel BJ, Matei DE, Li Y, Sun K, Luptakova K, Matulonis UA and Monk BJ. Niraparib monotherapy for late-line treatment of ovarian cancer (QUADRA): a multicentre, open-label, single-arm, phase 2 trial. Lancet Oncol 2019; 20: 636-648.

[3] Ray-Coquard I, Pautier P, Pignata S, Pérol D, González-Martín A, Berger R, Fujiwara K, Vergote I, Colombo N, Mäenpää J, Selle F, Sehouli J, Lorusso D, Guerra Alía EM, Reinthaller A, Nagao S, Lefeuvre-Plesse C, Canzler U, Scambia G, Lortholary A, Marmé F, Combe P, de Gregorio N, Rodrigues M, Buderath P, Dubot C, Burges A, You B, Pujade-Lauraine E and Harter P; PAOLA-1 Investigators. Olaparib plus bevacizumab as first-line maintenance in ovarian cancer. N Engl J Med 2019; 381: 2416-2428.

[4] González-Martín A, Pothuri B, Vergote I, DePont Christensen R, Graybill W, Mirza MR, McCormick C, Lorusso D, Hoskins P, Freyer G, Baumann K, Jardon K, Redondo A, Moore RG, Vulsteke C, O'Cearbhaill RE, Lund B, Backes F, Barretina-Ginesta P, Haggerty AF, Rubio-Pérez MJ, Shahin MS, Mangili G, Bradley WH, Bruchim I, Sun K, Malinowska IA, Li Y, Gupta D and Monk BJ; PRIMA/ENGOT-OV26/GOG-3012 Investigators. Niraparib in patients with newly diagnosed advanced ovarian cancer. N Engl J Med 2019; 381: 2391-2402.

[5] Cancer Genome Atlas Research Network. Integrated genomic analyses of ovarian carcinoma. Nature 2011; 474: 609-615.

[6] Casolino R, Paiella S, Azzolina D, Beer PA, Corbo V, Lorenzoni G, Gregori D, Golan T, Braconi C, Froeling FEM, Milella M, Scarpa A, Pea A, Malleo G, Salvia R, Bassi C, Chang DK and Biankin AV. Homologous recombination deficiency in pancreatic cancer: a systematic review and prevalence meta-analysis. J Clin Oncol 2021; 39: 2617-2631.

[7] Tlemsani C, Takahashi N, Pongor L, Rajapakse VN, Tyagi M, Wen X, Fasaye GA, Schmidt KT, Desai P, Kim C, Rajan A, Swift S, Sciuto L, Vilimas R, Webb S, Nichols S, Figg WD, Pommier Y, Calzone K, Steinberg SM, Wei JS, Guha U, Turner CE, Khan J and Thomas A. Whole-exome sequencing reveals germline-mutated small cell lung cancer subtype with favorable response to DNA repair-targeted therapies. Sci Transl Med 2021; 13: eabc7488.

[8] Landen C, Molinero L, Sehouli J, Miller A, Moore K, Taskiran C, Bookman M, Lindemann K, Anderson C, Berger R, Myers T, Beiner M, Reid T, Van Nieuwenhuysen E, Green A, Okamoto A, Aghajanian C, Thaker P, Blank S, Khor V, Wu F, Lin Y and Pignata S. Association of BRCA1/2, homologous recombination deficiency, and PD-L1 with clinical outcomes in patients receiving atezolizumab versus placebo combined with carboplatin, paclitaxel, and bevacizumab for newly diagnosed ovarian cancer: exploratory analyses of IMagyn050/GOG3015/ENGOT-ov39. Gynecol Oncol 2021; 162: S37-S38.

[9] Konstantinopoulos PA, Waggoner S, Vidal GA, Mita M, Moroney JW, Holloway R, Van Le L, Sachdev JC, Chapman-Davis E, Colon-Otero G, Penson RT, Matulonis UA, Kim YB, Moore KN, Swisher EM, Färkkilä A, D'Andrea A, Stringer-Reasor E, Wang J, Buerstatte N, Arora S, Graham JR, Bobilev D, Dezube BJ and Munster P. Single-arm phases 1 and 2 trial of niraparib in combination with pembrolizumab in patients with recurrent platinum-resistant ovarian carcinoma. JAMA Oncol 2019; 5: 1141-1149.

[10] Ding L, Kim HJ, Wang Q, Kearns M, Jiang T, Ohlson CE, Li BB, Xie S, Liu JF, Stover EH, Howitt BE, Bronson RT, Lazo S, Roberts TM, Freeman GJ, Konstantinopoulos PA, Matulonis UA and Zhao JJ. PARP inhibition elicits STING-dependent antitumor immunity in brca1-deficient ovarian cancer. Cell Rep 2018; 25: 2972-2980, e5.

[11] Kato K, Omura H, Ishitani R and Nureki O. Cyclic GMP-AMP as an endogenous second messenger in innate immune signaling by cytosolic DNA. Annu Rev Biochem 2017; 86: 541-566.

[12] Liu S, Cai X, Wu J, Cong Q, Chen X, Li T, Du F, Ren J, Wu YT, Grishin NV and Chen ZJ. Phosphorylation of innate immune adaptor proteins MAVS, STING, and TRIF induces IRF3 activation. Science 2015; 347: aaa2630.

[13] Sun L, Wu J, Du F, Chen X and Chen ZJ. Cyclic GMP-AMP synthase is a cytosolic DNA sensor that activates the type I interferon pathway. Science 2013; 339: 786-791.

[14] Khoo LT and Chen LY. Role of the cGAS-STING pathway in cancer development and oncotherapeutic approaches. EMBO Rep 2018; 19: e46935.

[15] Mariathasan S, Turley SJ, Nickles D, Castiglioni A, Yuen K, Wang Y, Kadel EE III, Koeppen H, Astarita JL, Cubas R, Jhunjhunwala S, Banchereau R, Yang Y, Guan Y, Chalouni C, Ziai J, Şenbabaoğlu Y, Santoro S, Sheinson D, Hung J, Giltnane JM, Pierce AA, Mesh K, Lianoglou S, Riegler J, Carano RAD, Eriksson P, Höglund M, Somarriba L, Halligan DL, van der Heijden MS, Loriot Y, Rosenberg JE, Fong L, Mellman I, Chen DS, Green M, Derleth C, Fine GD, Hegde PS, Bourgon R and Powles T. TGFβ attenuates tumour response to PD-L1 blockade by contributing to exclusion of T cells. Nature 2018; 554: 544-548.

[16] Ru B, Wong CN, Tong Y, Zhong JY, Zhong SSW, Wu WC, Chu KC, Wong CY, Lau CY, Chen I, Chan NW and Zhang J. TISIDB: an integrated repository portal for tumor-immune system interactions. Bioinformatics 2019; 35: 4200-4202.

[17] Takaya H, Nakai H, Takamatsu S, Mandai M and Matsumura N. Homologous recombination deficiency status-based classification of high-grade serous ovarian carcinoma. Sci Rep 2020; 10: 2757.

[18] Ritchie ME, Phipson B, Wu D, Hu Y, Law CW, Shi W and Smyth GK. Limma powers differential expression analyses for RNA-sequencing and microarray studies. Nucleic Acids Res 2015; 43: e47.

[19] R Core Team (2020). R: A language and environment for statistical computing. R Foundation for Statistical Computing, Vienna, Austria. Available from: https://www.R-project.org/.

[20] Yu G, Wang LG, Han Y and He QY. clusterProfiler: an R package for comparing biological themes among gene clusters. OMICS 2012; 16: 284-287.

[21] Chalmers ZR, Connelly CF, Fabrizio D, Gay L, Ali SM, Ennis R, Schrock A, Campbell B, Shlien A, Chmielecki J, Huang F, He Y, Sun J, Tabori U, Kennedy M, Lieber DS, Roels S, White J, Otto GA, Ross JS, Garraway L, Miller VA, Stephens PJ and Frampton GM. Analysis of 100,000 human cancer genomes reveals the landscape of tumor mutational burden. Genome Med 2017; 9: 34.

[22] Hao Y, Hao S, Andersen-Nissen E, Mauck WM 3rd, Zheng S, Butler A, Lee MJ, Wilk AJ, Darby C, Zager M, Hoffman P, Stoeckius M, Papalexi E, Mimitou EP, Jain J, Srivastava A, Stuart T, Fleming LM, Yeung B, Rogers AJ, McElrath JM, Blish CA, Gottardo R, Smibert P and Satija R. Integrated analysis of multimodal single-cell data. Cell 2021; 184: 3573-3587, e29.

[23] Zhang X, Lan Y, Xu J, Quan F, Zhao E, Deng C, Luo T, Xu L, Liao G, Yan M, Ping Y, Li F, Shi A, Bai J, Zhao T, Li X and Xiao Y. CellMarker: a manually curated resource of cell markers in human and mouse. Nucleic Acids Res 2019; 47: D721-D728.

[24] Han X, Wang R, Zhou Y, Fei L, Sun H, Lai S, Saadatpour A, Zhou Z, Chen H, Ye F, Huang D, Xu Y, Huang W, Jiang M, Jiang X, Mao J, Chen Y, Lu C, Xie J, Fang Q, Wang Y, Yue R, Li T, Huang H, Orkin SH, Yuan GC, Chen M and Guo G. Mapping the mouse cell atlas by microwell-seq. Cell 2018; 172: 1091-1107, e17.

[25] Yoshihara K, Shahmoradgoli M, Martínez E, Vegesna R, Kim H, Torres-Garcia W, Treviño V,

Shen H, Laird PW, Levine DA, Carter SL, Getz G, Stemke-Hale K, Mills GB and Verhaak RG. Inferring tumour purity and stromal and immune cell admixture from expression data. Nat Commun 2013; 4: 2612.
[26] Wickham H. Ggplot2: Elegant Graphics for Data Analysis. 2nd Edition. New York: S-V; 2018.
[27] Adler D and Kelly ST (2020). Vioplot: violin plot. R package version 0.3.7. Available from: https://github.com/TomKellyGenetics/vioplot.
[28] Wei TY and Simko V (2021). R package 'corrplot': Visualization of a Correlation Matrix (Version 0.92). Available from: https://github.com/taiyun/corrplot.
[29] Miller RE, Leary A, Scott CL, Serra V, Lord CJ, Bowtell D, Chang DK, Garsed DW, Jonkers J, Ledermann JA, Nik-Zainal S, Ray-Coquard I, Shah SP, Matias-Guiu X, Swisher EM and Yates LR. ESMO recommendations on predictive biomarker testing for homologous recombination deficiency and PARP inhibitor benefit in ovarian cancer. Ann Oncol 2020; 31: 1606-1622.
[30] Foo T, George A and Banerjee S. PARP inhibitors in ovarian cancer: an overview of the practice-changing trials. Genes Chromosomes Cancer 2021; 60: 385-397.
[31] Shen J, Zhao W, Ju Z, Wang L, Peng Y, Labrie M, Yap TA, Mills GB and Peng G. PARPi triggers the STING-dependent immune response and enhances the therapeutic efficacy of immune checkpoint blockade independent of BRCAness. Cancer Res 2019; 79: 311-319.
[32] Parkes EE, Walker SM, Taggart LE, McCabe N, Knight LA, Wilkinson R, McCloskey KD, Buckley NE, Savage KI, Salto-Tellez M, McQuaid S, Harte MT, Mullan PB, Harkin DP and Kennedy RD. Activation of STING-dependent innate immune signaling By S-phase-specific DNA damage in breast cancer. J Natl Cancer Inst 2016; 109: djw199.
[33] Li XD, Wu J, Gao D, Wang H, Sun L and Chen ZJ. Pivotal roles of cGAS-cGAMP signaling in antiviral defense and immune adjuvant effects. Science 2013; 341: 1390-1394.
[34] Dangaj D, Bruand M, Grimm AJ, Ronet C, Barras D, Duttagupta PA, Lanitis E, Duraiswamy J, Tanyi JL, Benencia F, Conejo-Garcia J, Ramay HR, Montone KT, Powell DJ Jr, Gimotty PA, Facciabene A, Jackson DG, Weber JS, Rodig SJ, Hodi SF, Kandalaft LE, Irving M, Zhang L, Foukas P, Rusakiewicz S, Delorenzi M and Coukos G. Cooperation between constitutive and inducible chemokines enables T cell engraftment and immune attack in solid tumors. Cancer Cell 2019; 35: 885-900, e10.
[35] Nagarsheth N, Wicha MS and Zou W. Chemokines in the cancer microenvironment and their relevance in cancer immunotherapy. Nat Rev Immunol 2017; 17: 559-572.
[36] Li T, Fu J, Zeng Z, Cohen D, Li J, Chen Q, Li B and Liu XS. TIMER2.0 for analysis of tumor-infiltrating immune cells. Nucleic Acids Res 2020; 48: W509-W514.
[37] Raines LN, Zhao H, Wang Y, Chen HY, Gallart-Ayala H, Hsueh PC, Cao W, Koh Y, Alamonte-Loya A, Liu PS, Ivanisevic J, Lio CJ, Ho PC and Huang SC. PERK is a critical metabolic hub for immunosuppressive function in macrophages. Nat Immunol 2022; 23: 431-445.
[38] Anderson NR, Minutolo NG, Gill S and Klichinsky M. Macrophage-based approaches for cancer immunotherapy. Cancer Res 2021; 81: 1201-1208.
[39] James NE, Woodman M and Ribeiro JR. Prognostic immunologic signatures in epithelial ovarian cancer. Oncogene 2022; 41: 1389-1396.
[40] Du Y, Peng Q, Cheng D, Pan T, Sun W, Wang H, Ma X, He R, Zhang H, Cui Z, Feng X, Liu Z, Zhao T, Hu W, Shen L, Jiang W, Gao N, Martin BN, Zhang CJ, Zhang Z and Wang C. Cancer cell-expressed BTNL2 facilitates tumour immune escape via engagement with IL-17A-producing γδ T cells. Nat Commun 2022; 13: 231.
[41] Tothill RW, Tinker AV, George J, Brown R, Fox SB, Lade S, Johnson DS, Trivett MK, Etemadmoghadam D, Locandro B, Traficante N, Fereday S, Hung JA, Chiew YE, Haviv I; Australian Ovarian Cancer Study Group, Gertig D, DeFazio A and Bowtell DD. Novel molecular subtypes of serous and endometrioid ovarian cancer linked to clinical outcome. Clin Cancer Res 2008; 14: 5198-5208.
[42] Zheng J, Mo J, Zhu T, Zhuo W, Yi Y, Hu S, Yin J, Zhang W, Zhou H and Liu Z. Comprehensive elaboration of the cGAS-STING signaling axis in cancer development and immunotherapy. Mol Cancer 2020; 19: 133.
[43] Hopfner KP and Hornung V. Molecular mechanisms and cellular functions of cGAS-STING signalling. Nat Rev Mol Cell Biol 2020; 21: 501-521.
[44] Mowat C, Mosley SR, Namdar A, Schiller D and Baker K. Anti-tumor immunity in mismatch repair-deficient colorectal cancers requires type I IFN-driven CCL5 and CXCL10. J Exp Med 2021; 218: e20210108.
[45] Zhang C, Shang G, Gui X, Zhang X, Bai XC and Chen ZJ. Structural basis of STING binding with and phosphorylation by TBK1. Nature 2019; 567: 394-398.
[46] Dentro SC, Leshchiner I, Haase K, Tarabichi M, Wintersinger J, Deshwar AG, Yu K, Rubanova Y, Macintyre G, Demeulemeester J, Vázquez-García I, Kleinheinz K, Livitz DG, Malikic S, Donmez N, Sengupta S, Anur P, Jolly C, Cmero M, Rosebrock D, Schumacher SE, Fan Y, Fittall M, Drews RM, Yao X, Watkins TBK, Lee J, Schlesner M, Zhu H, Adams DJ, McGranahan N,

Swanton C, Getz G, Boutros PC, Imielinski M, Beroukhim R, Sahinalp SC, Ji Y, Peifer M, Martincorena I, Markowetz F, Mustonen V, Yuan K, Gerstung M, Spellman PT, Wang W, Morris QD, Wedge DC and Van Loo P; PCAWG Evolution and Heterogeneity Working Group and the PCAWG Consortium. Characterizing genetic intra-tumor heterogeneity across 2,658 human cancer genomes. Cell 2021; 184: 2239-2254, e39.

[47] Gohil SH, Iorgulescu JB, Braun DA, Keskin DB and Livak KJ. Applying high-dimensional single-cell technologies to the analysis of cancer immunotherapy. Nat Rev Clin Oncol 2021; 18: 244-256.

[48] Hernández-Camarero P, López-Ruiz E, Marchal JA and Perán M. Cancer: a mirrored room between tumor bulk and tumor microenvironment. J Exp Clin Cancer Res 2021; 40: 217.

[49] Elia I and Haigis MC. Metabolites and the tumour microenvironment: from cellular mechanisms to systemic metabolism. Nat Metab 2021; 3: 21-32.

[50] Spranger S, Dai D, Horton B and Gajewski TF. Tumor-residing Batf3 dendritic cells are required for effector T cell trafficking and adoptive T cell therapy. Cancer Cell 2017; 31: 711-723, e4.

[51] Chow MT, Ozga AJ, Servis RL, Frederick DT, Lo JA, Fisher DE, Freeman GJ, Boland GM and Luster AD. Intratumoral activity of the CXCR3 chemokine system is required for the efficacy of Anti-PD-1 therapy. Immunity 2019; 50: 1498-1512, e5.

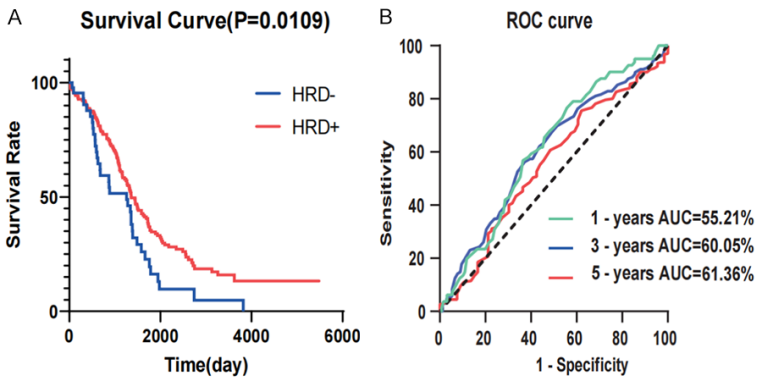

Supplementary Figure 1. A. Survival curves for HRD positive and HRD negative ovarian cancer. B. ROC curves for HRD score in the TCGA-OV cohort.